HYDROLOGICAL PROCESSES
Hydrol. Process. **22**, 941–953 (2008)
Published online 8 February 2008 in Wiley InterScience
(www.interscience.wiley.com) DOI: 10.1002/hyp.6984

Influence of hyporheic flow and geomorphology on temperature of a large, gravel-bed river, Clackamas River, Oregon, USA

Barbara K. Burkholder,[1] Gordon E. Grant,[2†] Roy Haggerty,[1]* Tarang Khangaonkar[3] and Peter J. Wampler[4]

[1] *Department of Geosciences, Oregon State University, 104 Wilkinson Hall, Corvallis OR 97331-5506 USA*
[2] *USDA Forest Service, Pacific Northwest Research Station, Corvallis OR 97331 USA*
[3] *Marine Sciences Laboratory, Pacific Northwest National Laboratory, Seattle WA 98382 USA*
[4] *Department of Geology, Grand Valley State University, Allendale MI 49401 USA*

Abstract:

The hyporheic zone influences the thermal regime of rivers, buffering temperature by storing and releasing heat over a range of timescales. We examined the relationship between hyporheic exchange and temperature along a 24-km reach of the lower Clackamas River, a large gravel-bed river in northwestern Oregon (median discharge = 75·7 m^3/s; minimum mean monthly discharge = 22·7 m^3/s in August 2006). With a simple mixing model, we estimated how much hyporheic exchange cools the river during hot summer months. Hyporheic exchange was primarily identified by temperature anomalies, which are patches of water that demonstrate at least a 1 °C temperature difference from the main channel. Forty hyporheic temperature anomalies were identified through field investigations and thermal-infrared-radiometry (TIR) in summer 2006. The location of anomalies was associated with specific geomorphic features, primarily bar channels and bar heads that act as preferential pathways for hyporheic flow. Detailed field characterization and groundwater modelling on three Clackamas gravel bars indicate residence times of hyporheic water can vary from hours to weeks and months. This was largely determined by hydraulic conductivity, which is affected by how recently the gravel bar formed or was reworked. Upscaling of modelled discharges and hydrologic parameters from these bars to other anomalies on the Clackamas network shows that hyporheic discharge from anomalies comprises a small fraction (≪1%) of mainstem discharge, resulting in small river-cooling effects (0·012 °C). However, the presence of cooler patches of water within rivers can act as thermal refugia for fish and other aquatic organisms, making the creation or enhancement of hyporheic exchange an attractive method in restoring the thermal regime of rivers. Copyright © 2008 John Wiley & Sons, Ltd.

KEY WORDS hyporheic exchange; river temperature; gravel bars; geomorphology; groundwater modelling

Received 15 October 2007; Accepted 11 December 2007

INTRODUCTION

Understanding heat fluxes within rivers is increasingly important as anthropogenic influences and changing climate alter river thermal regimes, which can lead to shifts in aquatic species composition and changing rates of biogeochemical processes (Evans *et al*., 1998; Poole and Berman, 2001). Numerous and inter-related physical mechanisms influence stream temperature, making it difficult to distinguish the magnitude or impact of individual drivers (Johnson, 2004).

Solar radiation (and shade), air temperature, groundwater inputs, and wind speed are the primary external drivers in most rivers that determine how much heat is added to or removed from the system (Sullivan and Adams, 1991). Internal drivers, which include bed conduction and hyporheic exchange, do not remove heat from the river channel but redistribute it temporally and spatially (Poole and Berman, 2001). Hyporheic exchange, where surface water enters the shallow subsurface (channel bed, banks or morphological features) and then reemerges back into the main channel, has previously been thought to have little impact on river temperature (Brown, 1969), but a number of recent studies show that hyporheic exchange plays an important role in the thermal dynamics of some streams (Story *et al*., 2003; Johnson, 2004; Loheide and Gorelick, 2006).

The hyporheic zone serves as transient storage within a river, where river water and heat can be retained for periods of time before being released back into the river (Bencala and Walters, 1983; Bencala, 2005). As surface water downwells into and is transported through the hyporheic zone, the heat within that water is transported and exchanged by several processes (Figure 1). Advection via fluid flow dominates heat transfer (Stallman, 1965; Silliman and Booth, 1993; Silliman *et al*., 1995; Anderson, 2005; Keery *et al*., 2006), although heat exchange may also influence hyporheic heat transfer. Along hyporheic flow paths, heat exchanges with sediment by conduction.

* Correspondence to: Roy Haggerty, Department of Geosciences, Oregon State University, 104 Wilkinson Hall, Corvallis OR 97331-5506 USA. E-mail: haggertr@geo.oregonstate.edu
† The contribution of Gordon E. Grant to this article was prepared as part of his official duties as a United States Federal Government employee.

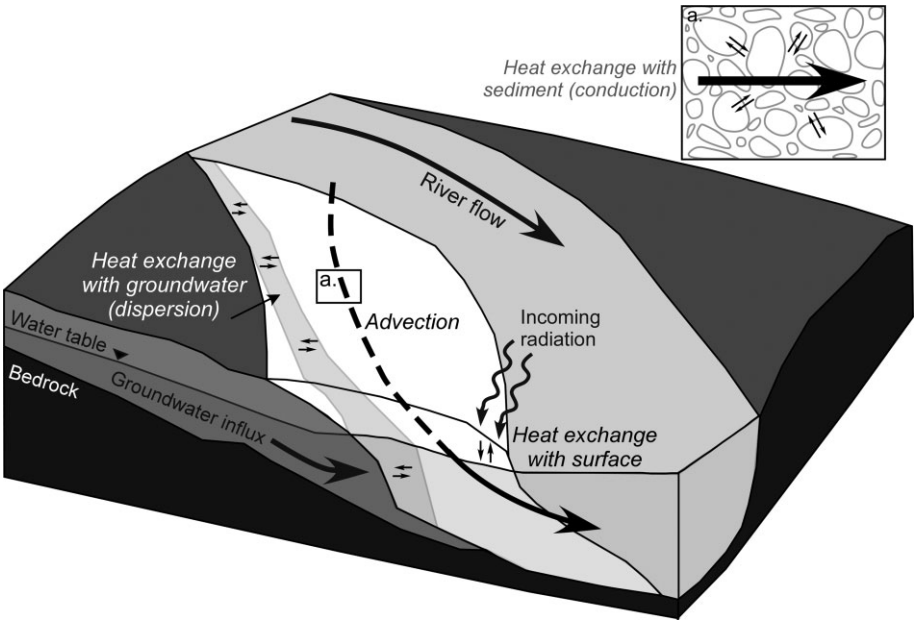

Figure 1. Conceptual diagram showing the different processes that influence hyporheic water temperatures in a gravel bar (white). Advection (large dashed/solid black arrow) transports heat via fluid flow, conduction (small black arrows) transfers heat between sediment and hyporheic water, dispersion and conduction (shaded zone within gravel bar) occur as hyporheic water and groundwater interact, and incoming solar radiation indirectly warms hyporheic water via conduction and transfer of latent and sensible heat

This exchange is fast—dimensional analysis for cobbles of typical properties indicate thermal equilibrium is achieved within 1 or 2 h. Heat also exchanges with groundwater by dispersion and conduction, and with the atmosphere by conduction and movement of latent and sensible heat. If the water table is high, solar heating of surface sediments may increase hyporheic water temperatures (Silliman *et al*., 1995; Arrigoni *et al., in press*). Collectively, these processes generally lead to a combination of 'buffering, cooling and lagging' (Arrigoni *et al., in press*) of temperatures within the hyporheic zone.

Emergent hyporheic temperature may be different from the mainstem temperature. Transport through the hyporheic zone may result in a temporal phase shift between hyporheic and mainstem temperatures, where cooler hyporheic water reemerges back into a warmer mainstem and vice versa. However, the mixing of emerging hyporheic water and mainstem water does not 'cool' a river—mean temperature may stay constant—but it does dampen diurnal temperature fluctuations in the river by decreasing maximum temperatures and increasing minimum temperatures (Johnson, 2004; Arrigoni *et al., in press*). This dampening results from shielding of hyporheic water from changes in solar radiation and air temperature that influence mainstem surface water temperature.

Hyporheic exchange can occur across several spatial scales, from roughness elements on the stream bed to channel-scale riffles and bars to reach-scale meander necks and floodplains (Edwards, 1998; Harvey and Wagner, 2000). Most hyporheic temperature studies to date have focused on examining the relationship between hyporheic exchange and channel-scale morphology. In smaller catchments, several studies report finding cooler water emerging from the bottom of riffles or step-pool structures (Evans and Petts, 1997; Brown *et al*., 2005; Hancock and Boulton, 2005; Moore *et al*., 2005; Sliva and Williams, 2005; Hunt *et al*., 2006). Peterson and Sickbert (2006) studied hyporheic exchange across a meander neck of a 3rd-order stream and found that hyporheic temperatures correlate with seasonal temperature variations, suggesting seasonal residence times. Fernald *et al*. (2000, 2006) reported on a larger river (8th order) that cooler water emerges from gravel bars into 'alcoves', or off-channel lentic water connected at the downstream end to the mainstem. Additionally, hyporheic flows were more pronounced and had a greater impact on river temperature where gravel had been recently reworked by river flows. Arscott *et al*. (2001) found that hyporheic exchange generated significant temperature heterogeneity in higher-order reaches (2–7th).

In reach-scale temperature studies, longitudinal trends in temperature demonstrate spatial and temporal thermal heterogeneity. Johnson (2004) compared bedrock and alluvial reaches along the same reach of 1st- and 2nd-order streams and found maximum daily temperatures were buffered by as much as 8·7 °C. Torgersen *et al*. (1999) used thermal imagery along a river reach and found that the general increase in temperature downstream contained several peaks and troughs, reflecting bedrock and alluvial reaches respectively.

There are few hyporheic temperature studies for larger, lower-gradient rivers, and none have quantified the effect of hyporheic exchange on overall longitudinal river temperature. In this study, we sought to: (1) identify areas of hyporheic exchange on a large,

DOI: 10.1002/hyp

gravel-bed river and investigate their relationship with channel morphological features, (2) quantify the amount of hyporheic exchange occurring, and (3) estimate how much hyporheic exchange affects overall river temperatures.

METHODS

Study area

The Clackamas River is a 6th-order, gravel-bed river in northwestern Oregon, USA that drains approximately 2430 km^2 from its headwaters in the Cascade Range to its confluence with the Willamette River in Oregon City. Our study focussed on a 24-km reach on the lower Clackamas River, stretching from River Mill Dam (River km (RKM) 37) to Carver, Oregon (RKM 13) (Figure 2). The dam location marks a change of topography within the drainage basin, with the river moving from a confined canyon into a broad valley. Longitudinal gradients below the dam along the study reach average 0·0029 (Wampler, 2004). The median annual flow is 75·7 m^3/s and the median summer flow is 25·9 m^3/s.

Sediment supply to the lower river is generated primarily from periglacial sediment in the Cascade Range. Dam infrastructure on the Clackamas has cut off this supply for almost 100 years, and sediment inputs into the reach are limited to periodic erosion of alluvial Holocene terraces (Wampler, 2004). However, an extensive gravel bar population (>50 bars) is distributed throughout the study reach, with median grain-size of 7·5 cm (Wampler, 2004). The population is composed primarily of mid-channel bars (55% of bars by area), with lateral bars (34%) and point bars (11%) making up the rest of the network. The bar alluvium, which can range up to 6 m in thickness, rests on cemented, fine-grained Miocene volcanoclastics and mudstones. The Sandy River Mudstone, which underlies the lower 21 km of the study reach, is easily eroded, leading to rapid formation of flutes and potholes when bedrock surfaces are exposed (Wampler, 2004).

Gravel bar stability decreases downstream, with well-vegetated, coarse-grained, skeletal bars, bars without finer sediments (median grain-size (D_{50}) surface: 15–30 cm), in the upper 3 km of the reach grading into unvegetated bars with smaller grain sizes (D_{50} surface = 5–7 cm). Wampler (2004) points out that the presence of the dam most likely causes this effect, as winter flows (850–1130 m^3/s) winnow out fines and smaller particles from the upper reaches and transport them downstream. Winter flows influence bar morphology throughout the reach, with most gravel reworking occurring between Feldheimer (RKM 30) and Carver (RKM 13).

The dam also affects the river temperature regime, especially during low flows in the summer months. The magnitude of this change has been modelled with CE-QUAL-W2, a hydrodynamic 2D water quality model, which shows that the Clackamas River currently exceeds state temperature standards by 1–3 °C from July to September (Portland General Electric, 2005). Current research in association with dam relicensing efforts are exploring natural mechanisms of thermal mitigation, including potential thermal benefits of adding gravel to

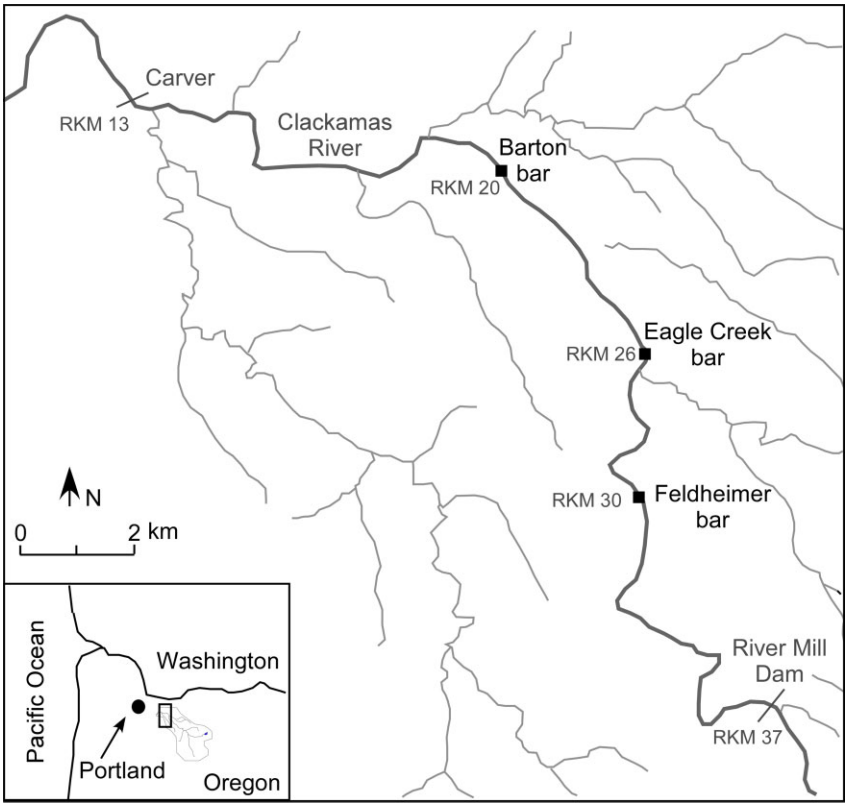

Figure 2. Site location and study reach, lower Clackamas River, Oregon, USA

DOI: 10.1002/hyp

the river to increase the amount of hyporheic exchange and hyporheic buffering.

Field measurements and data collection

Our field campaign from July to September 2006 investigated the gravel bars within the study reach, the hypothesized primary location of hyporheic flow that could influence mainstem river temperature. Owing to the length of the study reach, hyporheic exchange was identified using techniques that were easy to conduct and replicate over 24 km of river. During early reconnaissance, we identified locations with visually observable flow from gravel bars and used a handheld YSI 63 electrical conductivity and temperature probe (Yellow Springs, Ohio, USA) to identify temperature anomalies, which we defined as patches of water that deviate from mainstem water temperatures by at least 1 °C. The handheld probe was used to conduct temperature surveys around bar perimeters and identify anomaly locations. Reference mainstem temperatures were taken during temperature surveys at each site to account for diurnal heating of the river. Once an anomaly was identified, we also recorded its electrical conductivity and width and depth along gravel bar edges. Groundwater inputs were distinguished from hyporheic flow by: (1) water emerging from channel edges rather than gravel bars; (2) higher specific conductance (>80 μS/cm compared to river 55–65 μS/cm); (3) iron-stained sediment resulting from groundwater oxidation; and/or (4) consistent temperatures representative of groundwater (10–12 °C (well logs obtained from Oregon Water Resources Department (OWRD))). River discharge decreased throughout the summer (from 28 to 21 m^3/s), and to capture how this impacted the hyporheic zone, most identified anomaly sites were revisited several times over the summer to take more temperature measurements and re-measure anomaly dimensions.

Two thermal infrared radiometry (TIR) surveys were flown over the study reach on August 13th, 2006, one at 6 a.m. and the other at 3 p.m. (Watershed Sciences, Inc., Corvallis, Oregon, USA). This provided a complete 2D map of daily maximum and minimum river surface temperatures, as well as an additional visual method to observe and detect temperature anomalies. Longitudinal temperature profiles were constructed by taking the median temperature for each sampled image per river kilometre. In-stream temperature loggers, deployed throughout the study reach before the flights, were used to calibrate and verify the accuracy of TIR data. Pixel resolution of imagery is 0·9 m.

Three gravel bars with temperature anomalies were selected for detailed field characterization and modelling. These three representative bars exhibited geomorphic features and sedimentological textures characteristic of the majority of the gravel bar population on the lower Clackamas River. Field characterization included examination of bar type, location within the reach, sediment size, presence of vegetation, and bar history. On the basis of comparison of aerial photos from July 2005 (discharge, $Q = 29{\cdot}3$ m^3/s) and August 2006 ($Q = 23$ m^3/s), gravel features that did not appear in 2005 photos but were mapped in 2006 are considered 'new' features. We refer to all other features as older, but recognize that these bars also have a distribution of ages. Figure 3 shows basic bar morphology and interpreted hyporheic flow paths for each bar. Feldheimer bar (RKM 30) is an older, large lateral bar that is well-vegetated except for a 350-m long unvegetated back-bar channel that becomes active during high flow. Eagle Creek bar (RKM 26) is a new gravel feature that formed along an older bar edge during 2005 winter flows (Figure 4). Barton bar is a mid-channel bar (RKM 20) that has new infillings of gravel among older bar deposits (Figure 4).

Each bar was instrumented with several 3·4-cm inner diameter (1·33-in) galvanized steel piezometers (Maas Midwest Manufacturing, Huntley, Illinois, USA) with 17·8-cm (7-in) screens immediately above a conical drive point (three piezometers in Feldheimer bar, three in Eagle

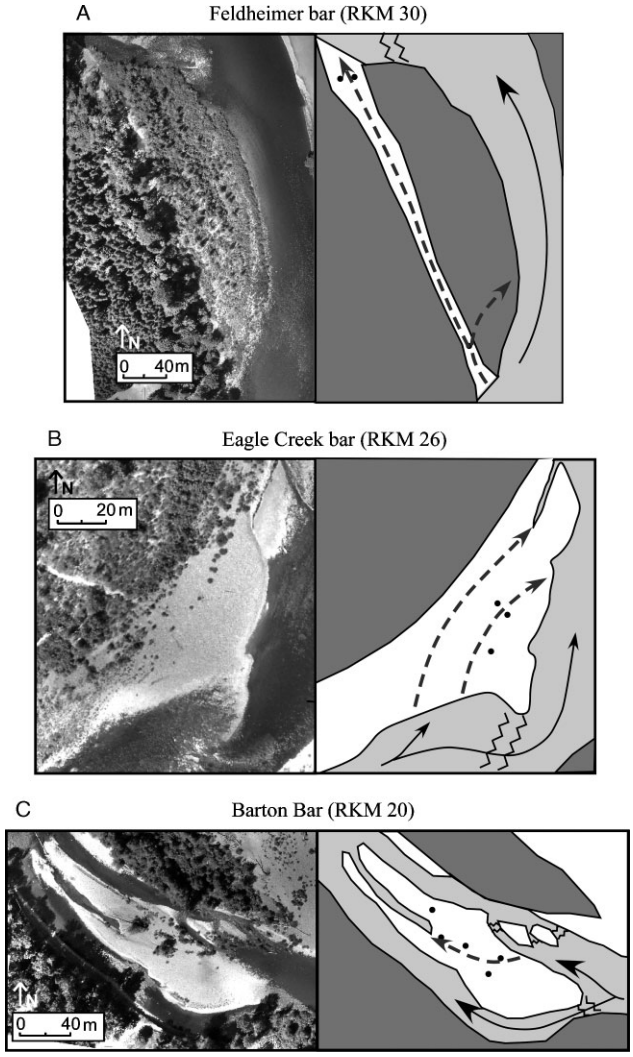

Figure 3. Summer 2006 aerial imagery and schematic diagram for (a) Feldheimer, (b) Eagle Creek, and (c) Barton gravel bars (see Figure 2 for locations). Piezometer locations (black dots) and interpreted subsurface flow paths (dashed grey lines) are overlain on open gravel (white) and vegetated areas (dark grey). Mainstem (light grey) flow direction given by solid black arrows. Riffles represented by zigzag pattern

DOI: 10.1002/hyp

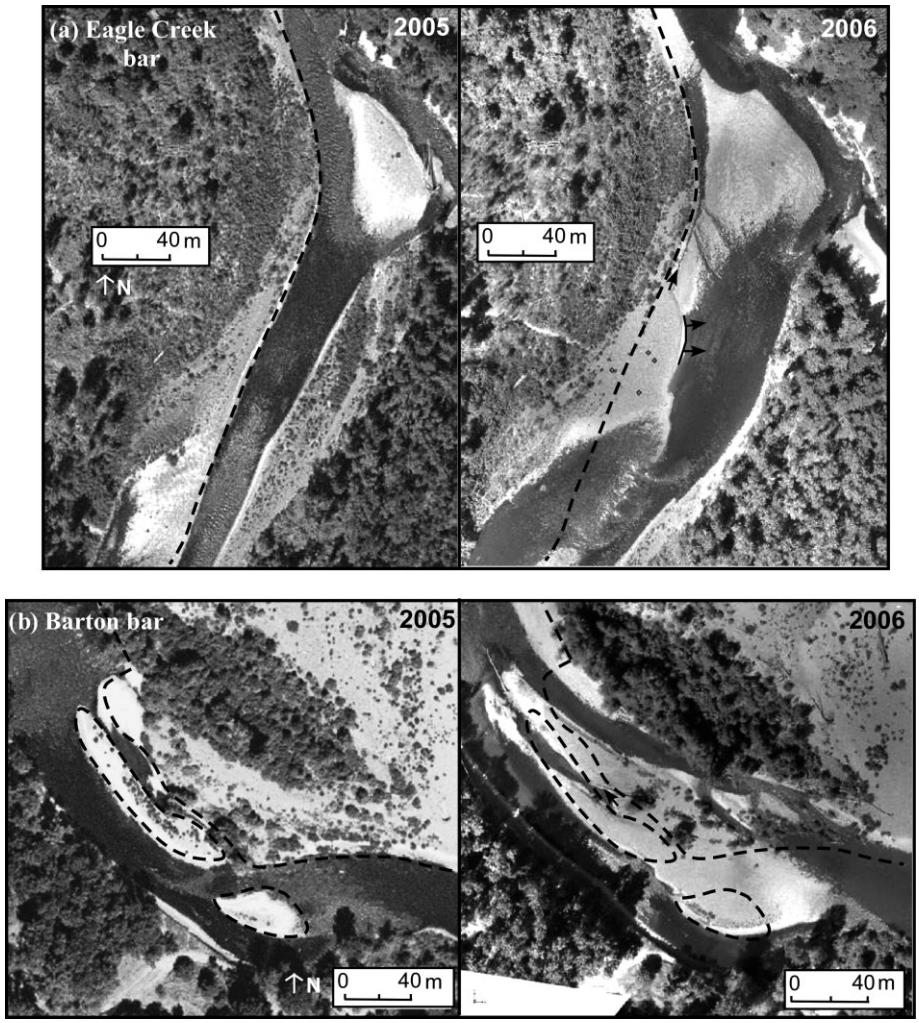

Figure 4. Aerial imagery showing gravel reworking between summers 2005 (left) and 2006 (right) for (a) Eagle Creek and (b) Barton bars. Dashed black lines follows outline of 2005 gravel bars and solid black arrows indicate flow direction of temperature anomalies

Creek bar, five in Barton bar). Given the large diameter of the sediment composing the gravel bars, it was not feasible to install the piezometers by hand-driven methods. A gas-powered jackhammer was used to drive the piezometers into the gravel bars, usually through at least 1 m of sediment to a depth of approximately 0·5 m beneath the water table. We assumed that flow across the gravel bars in the hyporheic zone is predominantly horizontal, which is hydrogeologically reasonable. Consequently, hydraulic head would have negligible changes with depth. Therefore, we put highest priority on horizontal separation of piezometers and did not install any multilevel piezometers. Alexander and MacQuarrie (2005) showed that temperature measurements within steel piezometers have less than 0·1 °C error and are perfectly correlated to *in situ* measurements.

Topographic surveys were conducted at each bar, using both a Leica TCRP 1201 total station (Heerbrugg, Switzerland) and a Trimble 4700 RTK GPS (Sunnyvale, California, USA). We mapped water edges, notable topographic features, and piezometer locations. Heads within piezometers were obtained through surveying the elevation of the top of the piezometer and subtracting the distance to the water table (2 cm vertical accuracy). Tidbit Stowaway thermistors (0·2 °C accuracy, Onset, Bourne, Massachusetts, USA) were checked against a 0·1 °C resolution NIST-traceable thermometer (Cole-Parmer, Vernon Hills, Illinois, USA) and placed within the screened section of the piezometers where they recorded temperature every 15 min for 7–10 days. Tidbits were also placed at head of the bar to record mainstem temperatures of water entering the bar and also placed in areas of emerging hyporheic flow. Slug tests were conducted within each piezometer, and results were analysed using methods outlined by Bouwer and Rice (1976) and Butler and Garnett (2000).

Model simulations of hyporheic exchange within gravel bars

Topographic surveys, slug tests, and temperature mapping from the selected gravel bars were used to build and parameterize steady-state groundwater flow models using MODFLOW (McDonald and Harbaugh, 1988) implemented via the GMS interface (Environmental Monitoring Systems, Inc., South Jordan, Utah, USA). Model domains were one-layer thick finite difference grids with

DOI: 10.1002/hyp

square cells, generally ranging between 0·2 and 0·5 m (depending on the size of the bar being modelled). Models were calibrated to water table elevations in piezometers and anomaly outflow dimensions. On two bars, residence time distributions from detailed Tidbit temperature surveys, simulated with the particle tracking package MODPATH (Pollack, 1994), were also used to calibrate the models. A flow-budget module within MODFLOW was used to calculate the hyporheic discharge emerging from the anomalies, and MODPATH provided a distribution of water residence times.

Upscaling hyporheic exchange to the reach scale

To assess how hyporheic exchange from gravel bars affects overall river temperatures, we calculated discharges for all anomalies interpreted to be driven by primarily hyporheic flow. We intentionally excluded anomalies that were interpreted to be because of groundwater. We estimated flux through each representative anomaly using Darcy's law ($Q_h = -K\nabla h\ A_h$). While technically valid at a point, we applied Darcy's law across temperature anomalies by assuming uniform parameters; the accuracy of this is discussed below. Q_h is hyporheic discharge (L^3/T) (as defined, it is a vector but we used only the magnitude), A_h is the cross-sectional area of the hyporheic discharge (L^2), K is the hydraulic conductivity of the sediment (L/T), and ∇h is hydraulic gradient (L/L). A_h was calculated by field measurement of the length across the edge of a gravel bar where we could detect a temperature difference and an estimate of the depth of gravel contributing to hyporheic flow. Hydraulic gradient across bars, in most cases, was measured in the field ($N = 27$). On bars, where hydraulic gradient was not directly measured ($N = 13$), we used the average of the field measurements of cross-bar gradients.

Using aerial photographs from 2005 and 2006, we estimated K for each anomaly based on how recently a gravel bar has been created or significantly reworked. From our observations, we assumed that new gravel bars or portions of pre-existing bars that formed during the previous year's high flows were likely to have a higher K than older bars, inferring that these deposits would not have been substantially infiltrated by fines. Older gravel bars, on the other hand, were interpreted as more likely to have had finer sediments infiltrating the sediment matrix, leading to lower K values (Packman and Salehin, 2003). Some bars are a combination of both older and newer gravel deposits, which can lead to large differences in K over a limited area. Model data from our three representative bars helped us constrain hydraulic conductivities by giving us a K estimate for newer and older bars, as well as bars with both newer and older deposits. The limitations of this approach will be discussed in the 'Results Section'.

We checked the accuracy of the Darcy's law discharge estimates against the discharge calculated by the groundwater flow models. We estimated parameters for Darcy's law using field estimates of average hydraulic gradient and hyporheic area. We also used a spatially-averaged K value from the groundwater models. Darcy's law and a full groundwater flow model yield nearly the same discharges: the relationship is approximately 1 : 1 and the mean difference between them is 25% (Figure 5). The discharges are nearly the same for the following reasons: changes in gradient (both direction and magnitude) along the flow paths are small; we assumed K and cross-sectional area of hyporheic discharge to be homogeneous along flow paths in both the Darcy's law and groundwater flow model calculations; and no sources or sinks of water exist along the flow paths. While there are significant heterogeneities in K within and between gravel bars, these within bar heterogeneities are at a large scale in comparison to the gravel bar, meaning that individual flow paths have relatively homogeneous K. Consequently, the Darcy's law approach provides a reasonable and feasible estimate of hyporheic discharge, and we confidently employ it for the other temperature anomalies on the Clackamas. All field and model data can be obtained from the appendices in Burkholder (2008).

RESULTS

Thermal infrared radiometry (TIR)

TIR was used to construct a reach-scale longitudinal profile of stream temperatures as recorded at two points in time (Figure 6). Comparison between thermal images and in-stream temperature loggers suggests that thermal images are within 0·5 °C of directly measured mainstem temperatures. Water released from the dam had a constant temperature of approximately 17·4 °C. Water warmed downstream during the day and cooled during the night, with rates of warming and cooling decreasing downstream, presumably because stream temperatures are closer to thermal equilibrium with the atmosphere and/or because increased discharge downstream (from groundwater and tributary inputs) creates a larger volume of water to be heated/cooled. Consequently, the warmest point in the reach during the day was near Barton (RKM 21), which approximately corresponds to the distance

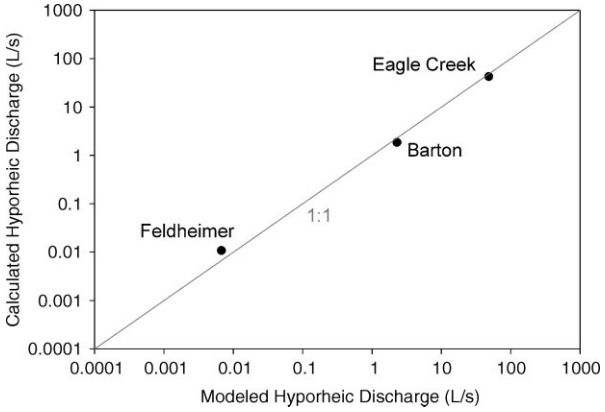

Figure 5. Comparison of calculated (Darcy's law) and modelled (MODFLOW) hyporheic discharge for temperature anomalies on gravel bars. For reference, 1 : 1 line is shown

DOI: 10.1002/hyp

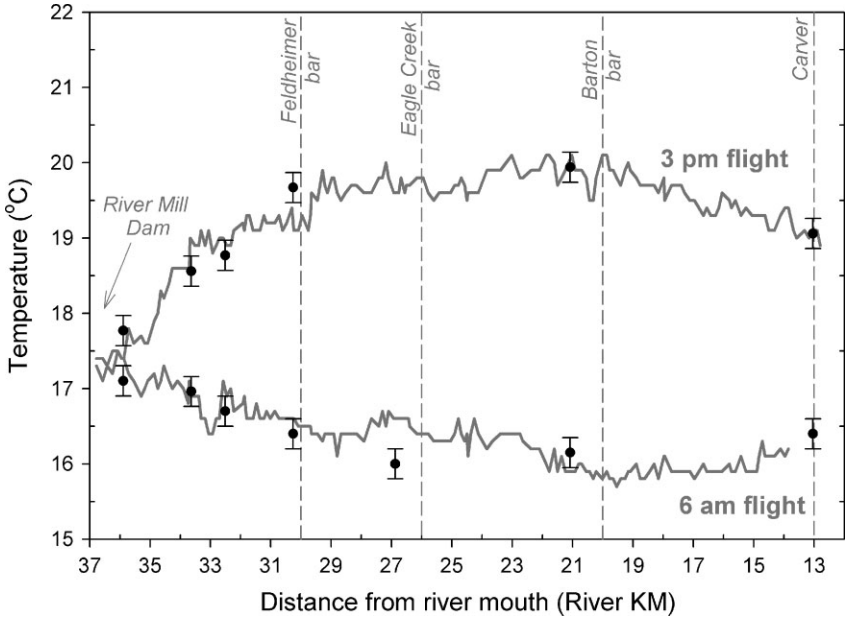

Figure 6. Longitudinal temperature profiles of the lower Clackamas River from River Mill Dam (RKM 37) to Carver, Oregon (RKM 13) recorded by TIR on August 13th, 2006. In-stream data loggers (black circles) indicate river temperature with measurement error

water travelled in daylight hours from the dam (16 km) (see analysis in Khangaonkar and Yang, *in press*). Further downstream, water was cooler because this water travelled some distance downstream from the dam during the night. An inverse pattern was observable in the early morning, with minimum temperatures recorded at Barton (Figure 6). This modulation of temperature amplitudes below a dam is well documented (Polehn and Kinsel, 1997; Lowney, 2000) and was recently revisited for the Clackamas River by Khangaonkar and Yang (*in press*).

TIR demonstrates that significant spatial and temporal thermal heterogeneity exists within the study reach. TIR morning imagery detected 34 temperature anomalies using the 1 °C rule, 16 of which were not previously identified in the field. These warmer patches of water emerged from gravel bars into a cooler mainstem (Figures 7, 8). Anomalies with temperatures cooler than the mainstem were also detected in morning imagery, suggestive of groundwater influx rather than hyporheic exchange. Afternoon flight imagery was not useful in identifying cooler hyporheic patches. TIR measures temperatures at the surface, which masked the denser, cooler water that emerged below the warmer surface water surface. The resolution of the imagery may also play a role in masking anomalies by averaging the much warmer gravel shoreline with cooler water temperatures in a single pixel.

Bar geomorphology controls on hyporheic exchange

A total of 52 temperature anomalies were identified by a combination of field investigations and TIR imagery over summer 2006. Depending on the time of the day, these features discharged water that generally ranged from 1 to 4 °C different than the mainstem. The anomalies were distributed along the entire 24-km study reach, with the greatest anomaly density (3·0 anomalies/km) in the 6·4-km reach between the Eagle Creek confluence to just below Barton (RKM 26·4 to RKM 20). The lowest density (1·4 anomalies/km) was in the 8-km reach immediately below River Mill Dam. This is consistent with previously interpreted levels of bar activity and presence of skeletal bars (bars without finer gravel) in the reaches immediately below the dam (Wampler, 2004).

Twelve anomalies were interpreted as primarily to be due to groundwater seepage rather than hyporheic exchange, based on the criteria outlined in methods. The remaining 40 anomalies are interpreted to be primarily driven by downwelling of river water, although we recognize they may also be influenced by some heat exchange with groundwater. This is supported by the fact that groundwater and hyporheic anomalies tended to occur adjacent to one another on individual gravel bars (6 of 12 identified groundwater seeps). One anomaly demonstrated warmer temperatures in the late afternoon, but the water table was near the uppermost gravel surface and was likely influenced by the heat of the gravel.

All hyporheic temperature anomalies occur on the edges of gravel bars. However, in most cases, they do not extend across the entire downstream edge of a gravel bar. Instead, they occur in association with specific geomorphic features present on gravel bars, features whose hydraulic gradient and hydraulic conductivity promote hyporheic residence times that result in offset hyporheic and mainstem temperature signals.

Twenty-four hyporheic anomalies (60%) occur at the downstream end of bar channels, which are unvegetated pathways that are active during high flows (e.g. Feldheimer and Barton bars). These channels occurred along the back margin of bars (i.e. away from the mainstem), across bars, or as paleochannels that have been infilled by new gravel. Gradients along bar channels were higher than the longitudinal river gradient (mean cross-bar gradient 0·007, compared to mean longitudinal

DOI: 10.1002/hyp

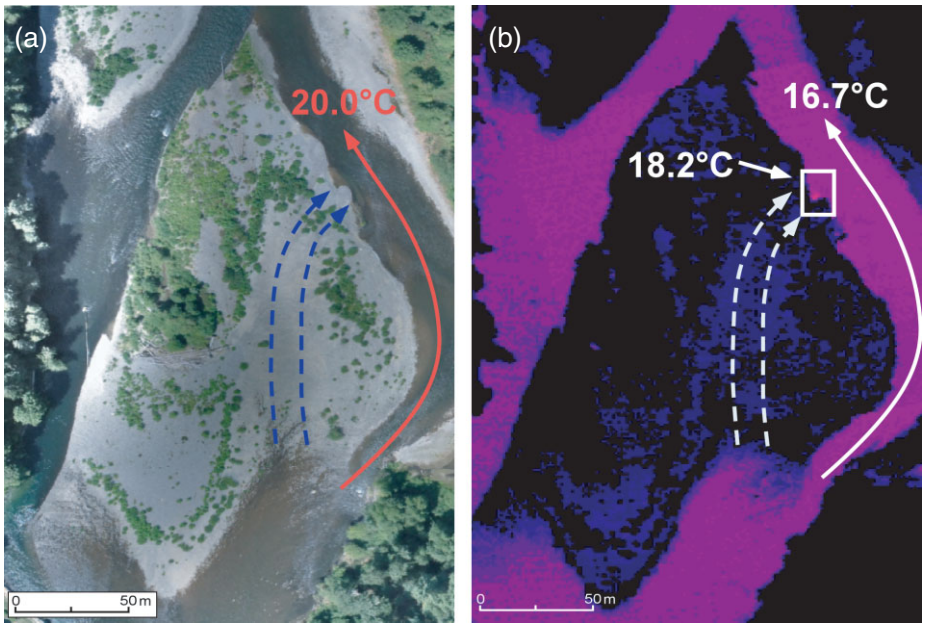

Figure 7. Hyporheic exchange across a mid-channel bar (RKM 27). (a) Dashed arrows on 2006 aerial photography indicate likely hyporheic flow paths through cross-bar channel feature. (b) Small, discrete temperature anomaly identified on 6 a.m. TIR photography

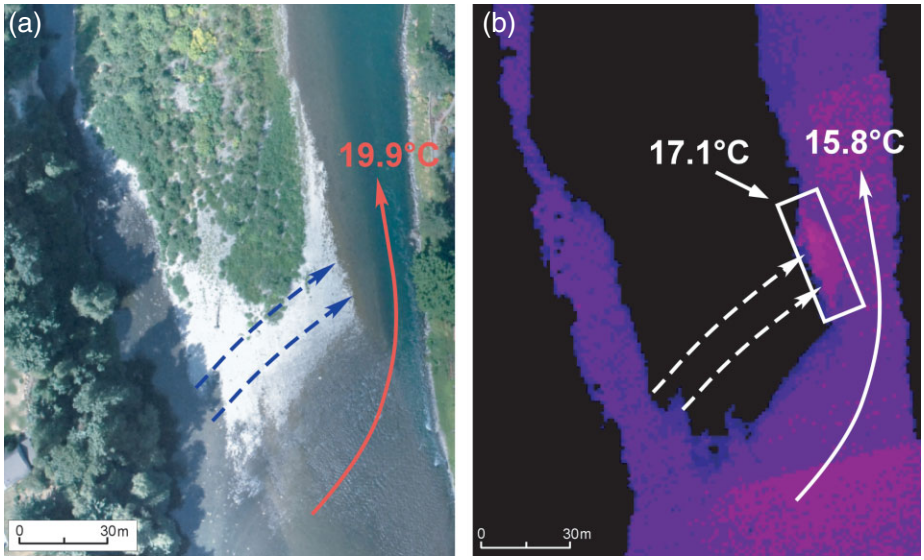

Figure 8. Hyporheic exchange across unvegetated section of mid-channel bar (RKM 15). (a) Dashed arrows indicate likely hyporheic flow paths through bar head feature. (b) Laterally extensive temperature anomaly identified on TIR 6 a.m. photography

gradient 0·0029). Temperature anomalies associated with bar channels formed discrete, small patches (<0·5 to 1 m in length as measured along the bar margin) due to the more defined structure of the feature (Figure 7).

Sixteen hyporheic anomalies (40%) were located downstream from bar heads, where hyporheic exchange follows a cross-bar gradient from hydraulically pooled water at the bar head to upwelling at the bar tail. (e.g. Eagle Creek bar) (Figure 8). Unlike bar channels, we interpret hyporheic flow through this geomorphic feature as not being confined to discrete subsurface channels, but occurring across riffle structures, large sections of bars, or entire bars. Downstream temperature anomalies associated with this feature were laterally extensive (up to 25 m along gravel bar edges). Bar heads were primarily found on mid-channel bars, where branching of the mainstem creates higher hydraulic gradients (0·005–0·012) because of elevation differences between channels.

Decreases in river discharge throughout the summer, particularly from July to August, did influence the size of temperature anomalies. Generally, as discharge decreased, the width of several temperature anomalies along gravel bar edges also decreased (up to 1–2 m). However, all except two hyporheic anomalies persisted through late July and August when river temperatures were highest in the channel.

Bar-scale data and model analysis

We summarize field and model data for each of the gravel bars selected for further characterization in

DOI: 10.1002/hyp

Table I. Field and model data for representative Clackamas gravel bars

Parameter	Feldheimer bar RKM 30	Eagle Creek bar RKM 26	Barton bar RKM 20
Bar type	Lateral	Point Bar	Mid-channel
Geomorphic feature	Back-bar channel	Bar head	Remnant channel
Gradient (m/m)	0·010	0·012	0·015
D_{50} surface (cm)	6·4	5·8	6·9
D_{50} subsurface (cm)	1·2	3·4	2·2
Hyporheic area (m^2)	34	66	8
Geometric mean K (m/s)	$1{\cdot}99 \times 10^{-5}$	$6{\cdot}19 \times 10^{-2}$	$1{\cdot}93 \times 10^{-3}$
ln(K) variance	0·09	0·37	5·77
Residence time (d)	~1040	0·49	~12
Discharge (m^3/s)	$6{\cdot}73 \times 10^{-6}$	$4{\cdot}28 \times 10^{-2}$	$1{\cdot}85 \times 10^{-4}$

Table I. Changes in piezometer head elevations from upper to lower ends of the gravel bars varied, with about 0·1–0·2-m change across Eagle Creek and Barton bars and 0·682-m across the larger Feldheimer bar. Slug tests within piezometers demonstrated different behaviours between new and older gravel bars. In older bars (Feldheimer bar and sections of Barton bar), K ranges from $1{\cdot}1 \times 10^{-6}$ to $7{\cdot}7 \times 10^{-5}$ m/s. In gravel that had been recently reworked (Eagle Creek bar and sections of Barton bar), 5–10 s recovery to static water levels with atypical recovery curves made it difficult to assess hydraulic conductivity using established high-K slug test analysis methods. Estimates of K were obtained by calibrating the appropriate MODFLOW models to travel time measured in offset temperature fluctuations. Hydraulic-conductivity estimates average $6{\cdot}3 \times 10^{-2}$ m/s from the calibrated Eagle Creek bar model and $1{\cdot}9 \times 10^{-3}$ m/s from the calibrated Barton bar model.

Week-long temperature surveys also showed important differences between the older and newer gravel bars (Figure 9). Temperatures in Eagle Creek bar showed a diurnal variation in temperature. As water from the mainstem moves through the bar, diurnal peaks in temperature were reduced to 20% of their original peak height when they emerged back into the main channel, reflective of advective and conductive heat transfer. The phase lag in emerging hyporheic temperature indicates a 11·5–11·8 h water residence time, which approaches the maximum phase shift possible.

Temperature surveys from within Feldheimer and Barton bars did not fluctuate diurnally, but temperatures measured in down-gradient piezometers were cooler than in up-gradient piezometers (Figure 9). The lack of diurnal temperature fluctuations is more indicative of groundwater rather than hyporheic exchange, but water temperatures within the piezometers are well above ambient groundwater temperatures, suggesting that the water originated from the river channel. The loss of diurnal fluctuation is likely due to longer residence times (weeks to months), which is consistent with the much lower K values within the bars as estimated from slug tests and MODFLOW. Longer residence time can buffer and lag temperatures on a seasonal basis. For example, the temperature of emerging hyporheic water at Barton was consistently warmer than the mainstem channel in mid-September (Figure 9) because cloudy, cooler weather reduced the amount of heat gained by the mainstem. Groundwater contributions may still be significant in emerging hyporheic temperatures, especially on Feldheimer bar which is connected to the channel edge.

Estimates of discharge emerging from each temperature anomaly are dependent on hydraulic gradient, hyporheic cross-sectional area, and K (Table I). Of these variables, K has the most influence over hyporheic discharge. Eagle Creek bar, with the highest average K ($6{\cdot}19 \times 10^{-2}$ m/s) and largest hyporheic area (66 m^2), has the greatest calculated discharge of 42·5 L/s (0·0425 m^3/s), or 0·002% of the mainstem discharge. Feldheimer bar, with the lowest average K ($1{\cdot}99 \times 10^{-5}$ m/s) and relatively large hyporheic area (34 m^2), has the lowest discharge of 0·00673 L/s ($6{\cdot}73 \times 10^{-6}$ m^3/s), almost four orders of magnitude lower than Eagle Creek. Barton bar, with an intermediate K ($1{\cdot}93 \times 10^{-3}$ m/s) but small hyporheic area (8 m^2) has an anomaly discharge of 1·85 L/s ($1{\cdot}85 \times 10^{-4}$ m^3/s), which is two orders of magnitude lower than Eagle Creek.

Effect of hyporheic anomalies on river temperature

Estimates of K for the three representative bars were used to estimate K values for the larger population of hyporheic temperature anomalies, using an inferred association between recent gravel reworking and K. Using aerial photo analysis to assess the degree of gravel reworking that occurred on bars during 2005–2006 winter flows, we assigned an Eagle Creek K value of $6{\cdot}19 \times 10^{-2}$ m/s to new bars or bars that were extensively reworked, a Barton K value of $1{\cdot}93 \times 10^{-3}$ m/s to bars that showed some degree of reworking, and a Feldheimer K value of $1{\cdot}99 \times 10^{-5}$ m/s to older bars with little to no gravel reworking. We recognize that K is a highly variable and sensitive parameter, and our approach does not address downstream fining of sediments and changes in sediment packing. We view this approach as providing a rough estimate of the overall order-of-magnitude effect of anomaly-based hyporheic flow on stream temperatures that is consistent with the limited data available.

DOI: 10.1002/hyp

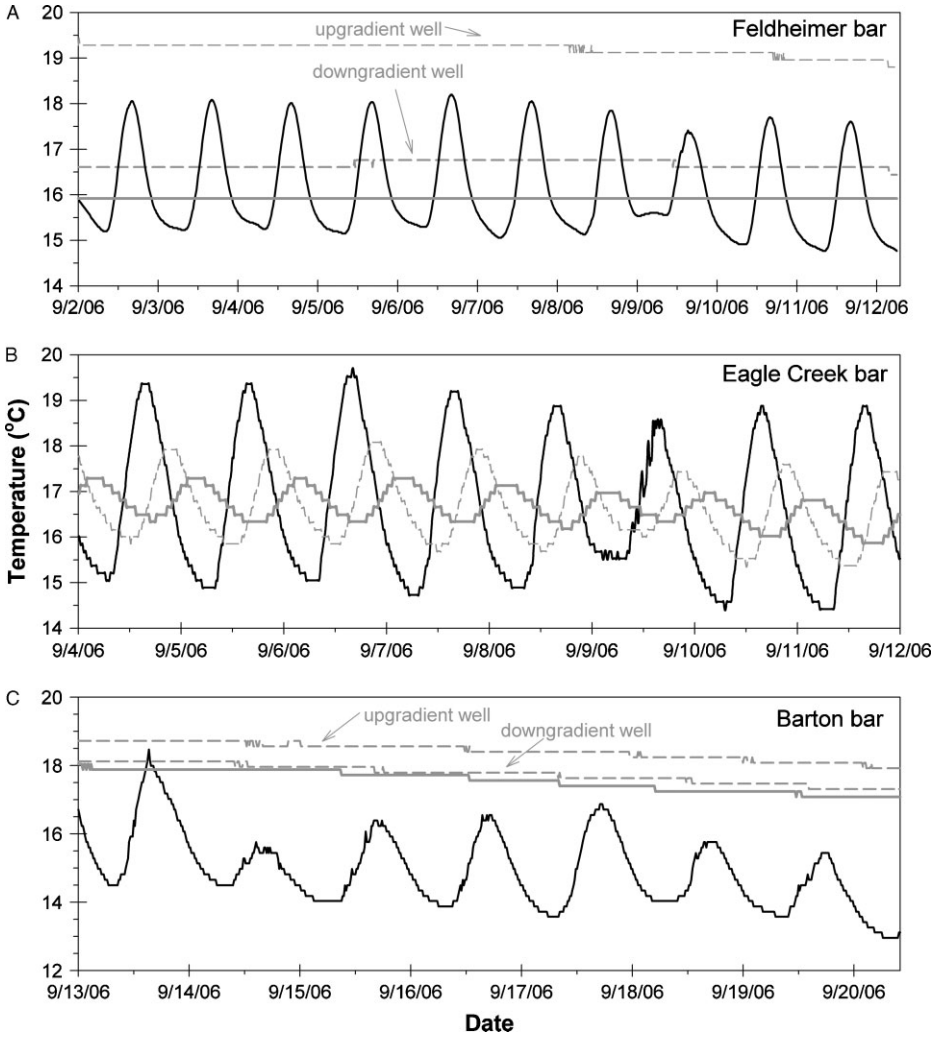

Figure 9. Week-long temperature profiles for (a) Feldheimer, (b) Eagle Creek, and (c) Barton bars. Surface mainstem temperatures (solid black lines) show dampening of diurnal fluctuations in emerging hyporheic flow (solid grey lines). Dashed grey lines represent within bar well temperatures

The change in river temperature because of hyporheic discharge can be approximated using a mixing equation

$$T_c = \frac{Q_m T_m + \sum (Q_h T_h)}{Q_c} \quad (1)$$

where Q_m is mainstem discharge (L^3/T), T_m is mainstem temperature (°C), Q_h is hyporheic discharge (L^3/T), T_h is hyporheic temperature (°C), Q_c is combined discharge (L^3/T), and T_c is combined river temperature (°C). This equation neglects other sources and sinks of heat, offsets in time due to travel time from one anomaly to the next, and dispersion. These effects are discussed below. We emphasize that we investigated only hyporheic exchange, and not the effects of groundwater inputs on river temperature, so groundwater seeps were not included. Solving for T_c and subtracting it from mainstem temperature, T_m, gives the amount of river cooling expected from hyporheic exchange. To check the accuracy of the mixing equation approach, we compared it to results from a 2D hydrodynamic temperature model of the lower Clackamas River. We used CE-QUAL-W2 (Cole and Wells, 2004), a 2D hydrodynamic model which incorporates the full spectrum of heat sources and sinks, to estimate river temperature sensitivity to hyporheic exchange. The CE-QUAL-W2 model was parameterized with a network of meteorological sensors that provided air temperature (two points), short- and long-wave radiation (one point), cloud cover (one point), wind speed (four points), and humidity (three points). Other details on the model are provided by Battelle (2004) and Khangaonkar and Yang (*in press*). We used anomaly discharge, residence time, and temperature from the Eagle Creek bar and added 40 additional Eagle Creek-like anomalies throughout the river (in effect, doubling the number of current hyporheic anomalies), maintaining the same degree of anomaly density between different stretches of river. The model estimates river cooling of 0·16 °C. Using the mixing model, we estimated the cooling associated with the Eagle Creek anomaly (0·006 °C) and to simulate gravel augmentation, multiplied that effect by 40. This gives a river-cooling estimate of 0·24 °C, an overestimate of 50%.

Using parameters shown in Table II, the mixing equation estimates that existing hyporheic anomaly-based

DOI: 10.1002/hyp

hyporheic discharge (0·07% of total mainstem discharge) provides a local cooling of the summer-time maximum daily temperature in lower Clackamas River by 0·012 °C.

DISCUSSION

We estimate that existing hyporheic flow in the Clackamas has a minimal impact on daily maximum temperature. This estimate is subject to three significant sources of uncertainty detailed below: the estimate of K; the calculation of discharge; and unaccounted for hyporheic exchange.

First, determining K for each of the gravel bars with temperature anomalies is difficult. We assigned K values using data from our three intensively studied bars to all anomalies in the study reach based on whether a bar was new, older, or a combination of new and older deposits. We do not know if this approach over- or underpredicts K values, but overall temperature effects in the mainstem are very sensitive to the assignment of K values. By way of sensitivity analysis, if all gravel bars are assigned the maximum measured value of K (Eagle Creek), the mixing model estimates an overall reduction in maximum daily temperatures in the summer of 2006 as 0·021 °C. If all gravel bars are assigned the minimum measured value of K (Feldheimer), the mixing model estimates a reduction in maximum daily temperatures of $7{\cdot}14 \times 10^{-6}$ °C.

Secondly, we used a simple mixing equation to estimate the effect of hyporheic discharge on mainstem temperature. The steady state simplification assumes that the cooling over multiple anomalies is cumulative and neglects decay and phase effects due to travel time (i.e. temperature is treated conservatively). This model may overestimate the temperature effect. Our comparison with CE-QUAL-W2, which accounts for longitudinal heat loss/gain, demonstrates that if we added 40 Eagle Creek bars on the lower Clackamas by gravel augmentation and make the same calculation with the mixing model as outlined above, the mixing model overestimates the cooling effect by 50%.

Finally, our study has focussed on quantifying hyporheic exchange over summer 2006 on gravel bars that consistently demonstrated different temperatures from the mainstem, because of buffering and lagging of heat resulting from advection and conduction. We did not quantify the thermal effects of diffuse hyporheic discharge through gravel bars where we did not detect a temperature difference, nor did we attempt to assign cooling associated with the simple downwelling of water into gravel bars (where water is not exposed to solar radiation or ambient air temperature). Also, we did not take other hyporheic spatial scales into account, including flow through submerged gravel bedforms (e.g. bed roughness elements), meander necks or floodplains. Exclusion of these effects underestimates the total amount of hyporheic cooling.

Table II. Numbers entered into mixing calculation

Parameter	Value	Source
Q_m	22·547 m^3/s	$Q_c - Q_h$
T_m	19·20 °C	Mean temperature for August 13, 2006
Q_h	0·153 m^3/s	Sum of all temperature anomaly discharges
T_h	Depends	T_m−magnitude of cooling for each anomaly
$\Sigma(Q_hT_h)$	2·660	
Q_c	22·7 m^3/s	USGS River Gauge at Estacada
T_c	19·187 °C	$Q_mT_m + \Sigma(Q_hT_h)/Q_c$
Cooling	0·012 °C	$T_m - T_c$

Reconciling these sources of error, which point in different directions, is difficult. Obtaining more refined estimates of K and hyporheic anomaly discharge would require building additional groundwater models for many more gravel bars on the lower Clackamas. Additional field studies and modelling exercises would examine other spatial scales of hyporheic flow and the thermal benefit afforded by water simply being shielded from solar radiation as it downwells into gravel.

Even within the constraints imposed by the uncertainties in our study, however, we believe our estimate of cooling is not likely to change drastically. Unlike smaller streams that may see several degrees of cooling from hyporheic buffering (Johnson, 2004), our results suggest that hyporheic exchange will cool larger rivers only a fraction of a degree. This is likely due to diminishing opportunities for hyporheic exchange as channel size increases (D'Angelo *et al*., 1993; Boulton *et al*., 1998). We found that in the Clackamas River, hyporheic discharge comprised only a fraction of mainstem summer discharge ($\ll$1%). It is therefore difficult for hyporheic exchange to exert significant effect on stream temperature, because any hyporheic buffering present is diluted by large mainstem discharges.

Although hyporheic discharge may not have a large effect on overall river temperature in a large river, we found that it can effectively create localized patches of water that have different temperatures from the mainstem. These patches increase thermal heterogeneity within the river channel and can provide thermal refugia (up to 4 °C cooler) for aquatic species that are stressed by conditions in the mainstem channel (Fernald *et al*., 2006 and Arscott *et al*., 2001).

Similar to previous studies (e.g. Kasahara and Wondzell, 2003; Poole *et al*., 2006), we found that channel-scale morphology controls hyporheic exchange in the Clackamas River, which in turn influences thermal heterogeneity (Arscott *et al*., 2001; Fernald *et al*., 2006). All anomalies were associated with gravel bars, with the largest discharges emerging from anomalies located downstream from bar heads. The largest number of anomalies were associated with bar channels, but these produced only modest hyporheic discharges.

In most cases, the link between channel morphology and hyporheic flow reflects morphologic control on the distribution and hydraulic properties of preferential flow paths in bars. Temperature anomalies were consistently

DOI: 10.1002/hyp

located downstream from observed or inferred flow paths, which are assumed to feed subsurface channels. Although these geomorphic features usually comprise only a fraction of a gravel bar's area, they generally have higher K values than other parts of the same bar (Wondzell and Swanson, 1999; Fernald *et al*., 2006). The bar channels and heads that had associated anomalies with the greatest hyporheic discharges had been reworked recently during recent high winter flows and presumably had fewer fines than older and less reworked parts of the bar. These older bar surfaces tended to be well-vegetated and have likely accumulated fines for longer periods of time. Our slug tests also suggested that K values can vary dramatically between newer and older bar features.

Bar channels and bar heads also have hydraulic gradients greater than the longitudinal river gradient because of downstream hydraulic controls and backwater effects. The slope transition at the head of the bar in effect acts as a broad-crested weir, slowing upstream flows. The water that does infiltrate the head of the bar will generally follow a shorter flow path directly through the bar; this will be the steepest gradient across the bar. Together, higher K and steeper hydraulic gradient create preferential flow paths, concentrating hyporheic flow. At Eagle Creek, we estimate that 76% of the total hyporheic flow in the bar was focused along a preferential flow path, giving rise to the downstream temperature anomaly.

On some bars, we found recently reworked bar channels and bar heads that appeared ideal candidates for preferential hyporheic flow, but no temperature anomaly was found. We speculate that in these cases hyporheic flow was present but in phase with mainstem temperature. For a maximum temperature difference to occur, the travel time across the bar must be $24(N - 1/2)$ h where N is a positive integer. A minimum temperature difference occurs, regardless of hyporheic discharge, at 24 N h. This means that certain bar sizes and K values can produce significant hyporheic flow but have no appreciable effect on the river temperature.

This study reveals the close coupling among channel morphology, hyporheic flow, and thermal heterogeneity. The relationship among these processes will be affected by channel dynamics in both natural rivers and those located downstream from dams or other anthropogenic influences. In the case of the Clackamas, long-term reduction in sediment supply and transport due to upstream dams has resulted in at least some reaches with limited gravel and skeletal coarse bars. The proposed artificial introduction of gravel to the river below the lowest dam has the potential to increase sediment transport, thereby affecting rates of bar construction, reworking, and channel migration. As per the results presented here, there should be at least some local effects on stream temperatures because of this increased channel activity. It remains to be seen what the magnitude and location of this effect is likely to be, but the opportunity to examine the relationships among channel morphology, stream temperature, and hyporheic flow represents an ideal field experiment.

CONCLUSIONS

Our field investigation identified 40 temperature anomalies over a 24-km reach on the lower Clackamas River, a low gradient, gravel-bed river. Temperature anomalies are the result of hyporheic exchange deviating from mainstem temperatures throughout the day, largely because of buffering and lagging of advected heat. The occurrence of temperature anomalies depends strongly on the presence of bar morphology. More specifically, hyporheic exchange that directly influences river temperature is associated with geomorphic features on bars like bar channels and bar heads that exhibit higher gradients (vs river gradient) and higher hydraulic conductivities. The flow emerging from these anomalies is largely controlled by the hydraulic conductivity of the sediments, meaning that gravel bars that have recently formed or been reworked will have greater hyporheic discharges.

A simple mixing model demonstrates that the overall cooling effect associated with these temperature anomalies is small (0·012 °C) because of the fact that hyporheic discharge emerging from these anomalies is only a small fraction (<0·07%) of mainstem discharge in a large river. However, these patches of cooler water can benefit cold-water species such as salmon, providing local habitat and refugia from warmer mainstem temperatures. With emerging interest in river restoration and incorporating natural river processes into restoration projects (Boulton, 2007), the creation or enhancement of cool patches resulting from hyporheic exchange is a viable method that could be used to offset the harmful effects of thermal degradation.

ACKNOWLEDGEMENTS

This material is based upon the work supported under a grant from Portland General Electric (PGE) and a cooperative agreement between Oregon State University and the USDA Forest Service. Any opinions, findings, and conclusions or recommendations expressed in this material are those of the authors and do not necessarily reflect the views of the supporting organizations. We thank Sarah Lewis for her support and expertise, Anne Jefferson for her contribution to the cooling calculation, the field team for their help and willingness to work long hours, and the PGE crew who took the time to shuttle our boat every day and offered technical support when needed. This manuscript benefited from the comments of two anonymous reviewers.

REFERENCES

Alexander MD, MacQuarrie KTB. 2005. The measurement of groundwater temperature in shallow piezometers and standpipes. *Canadian Geotechnical Journal* **42**: 1377–1390.

Anderson MP. 2005. Heat as a ground water tracer. *Ground Water* **43**: 951–968.

Arrigoni A, Poole GC, Mertes LAK, O'Daniel SJ, Woessner WW, Thomas SA. Buffering, lagging, or cooling? Disentangling mechanisms of hyporheic influence on stream channel temperature. *Water Resources Research* (in press).

Arscott DB, Tockner K, Ward JV. 2001. Thermal heterogeneity along a braided floodplain river (Tagliamento River, northeastern Italy). *Canadian Journal of Fisheries and Aquatic Science* **58**: 2359–2373.

Battelle. 2004. *Clackamas River Hydroelectric Project (FERC No. 2195) Water Quality Model of the Clackamas River, Appendix H, report to Portland General Electric*, 34.

Bencala KE. 2005. Hyporheic exchange flows. In *Encyclopedia of Hydrological Sciences*, Anderson MG (ed.). John Wiley and Sons: Chichester, UK; 1733–1740.

Bencala KE, Walters RA. 1983. Simulation of solute transport in a mountain pool-and-riffle stream: A transient storage model. *Water Resources Research* **19**: 718–724.

Boulton AJ. 2007. Hyporheic rehabilitation in rivers: restoring vertical connectivity. *Freshwater Biology* **52**: 632–650, DOI: 10·1111/j.1365–2427·2006·01710.x.

Boulton AJ, Findlay S, Marmonier P, Stanley EH, Valett HM. 1998. The functional significance of the hyporheic zone in streams and rivers. *Annual Review of Ecology and Systematics* **29**: 59–81, DOI: 10·1146/annurev.ecolsys.29·1·59.

Bouwer H, Rice RC. 1976. A slug test for determining hydraulic conductivity of unconfined aquifers with completely or partially penetrating wells. *Water Resources Research* **12**: 423–428.

Brown GW. 1969. Predicting temperatures of small streams. *Water Resources Research* **5**: 68–75.

Brown LE, Hannah DM, Milner AM. 2005. Spatial and temporal water column and streambed temperature dynamics within an alpine catchment: implications for benthic communities. *Hydrological Processes* **19**: 1585–1610.

Burkholder BK. 2008. *Influence of Hyporheic Flow and Geomorphology on Temperature of a Large, Gravel-bed River, Clackamas River, Oregon, USA*. MS Thesis. Oregon State University, Corvallis; 170 p.

Butler JJ Jr, Garnett EJ. 2000. Simple procedures of analysis of slug tests in formations of high hydraulic conductivity using spreadsheet and scientific graphics software. Kansas Geological Survey: Lawrence, Kansas, USA; KGS Open File Report 2000-40, http://www.krewg.org/Hydro/Publications/OFR00_4-/index.html [accessed February 15 2007].

Cole TM, Wells SA. 2004. CE-Qual-W2: a two-dimensional, laterally averaged, hydrodynamic and water quality model, Version 3·2. User Manual. Instruction Report E-95-1. U.S. Army Corps of Engineers: Washington, DC.

D'Angelo DJ, Webster JR, Gregory SV, Meyer JL. 1993. Transient storage in Appalachian and Cascade mountain streams as related to hydraulic characteristics. *Journal of the North American Benthological Society* **12**: 223–235.

Edwards RT. 1998. The hyporheic zone. In *River Ecology and Management: Lessons from the Pacific Coastal Ecoregion*, Naiman RJ, Bilby RE (eds). Springer Verlag: New York; 399–429.

Evans EC, Petts GE. 1997. Hyporheic temperature patterns within riffles. *Hydrological Processes* **42**: 199–213.

Evans EC, McGregor GR, Petts GE. 1998. River energy budgets with special reference to river bed processes. *Hydrological Processes* **12**: 575–595.

Fernald AG, Landers DH, Wigington PJ. 2000. Water quality effects of hyporheic processing in a large river. *International Conference on Riparian Ecology and Management in Multi-Land US Watersheds*. American Water Resources Association: Portland, Oregon, USA; 167–172.

Fernald AG, Landers DH, Wigington PJ. 2006. Water quality changes in hyporheic flow paths between a large gravel bed river and off-channel alcoves in Oregon, USA. *River Research and Applications* **22**: 1111–1124, DOI: 10·1002/rra.961.

Hancock PJ, Boulton AJ. 2005. The effects of an environmental flow release on water quality in the hyporheic zone of the Hunter River, Australia. *Hydrobiologia* **552**: 75–85.

Harvey JW, Wagner BJ. 2000. Quantifying hydrologic interactions between streams and their subsurface hyporheic zones. In *Streams and Ground Waters*, Jones JB, Mullholland PJ (eds). Academic Press: San Diego, CA; 425.

Hunt RJ, Strand M, Walker JF. 2006. Measuring groundwater-surface water interaction and its effect on wetland stream benthic productivity, Trout Lake watershed, northern Wisconsin, USA. *Journal of Hydrology* **320**: 370–384.

Johnson SL. 2004. Factors influencing stream temperatures in small streams: substrate effects and a shading experiment. *Canadian Journal of Fisheries and Aquatic Sciences* **61**: 913–923, DOI: 10·1139/F04-040.

Kasahara T, Wondzell SM. 2003. Geomorphic controls on hyporheic exchange flow in mountain streams. *Water Resources Research* **39**: 1005, DOI: 10·1029/2002WR001386.

Keery J, Binley A, Crook N, Smith JWN. 2006. Temporal and spatial variability of groundwater-surface water fluxes: development and application of an analytical method using temperature time series. *Journal of Hydrology* **336**: 1–16.

Khangaonkar T, Yang Z. Dynamic response of stream temperatures to boundary and inflow perturbation due to reservoir operations. *River Research and Applications* (in press).

Loheide SP II, Gorelick SM. 2006. Quantifying stream-aquifer interactions through the analysis of remotely sensed thermographic profiles and in situ temperature histories. *Environmental Science and Technology* **40**: 3336–3341, DOI: 10·1021/es0522074.

Lowney CL. 2000. Stream temperature variation in regulated rivers: evidence for a spatial pattern in daily minimum and maximum magnitudes. *Water Resources Research* **36**: 2947–2955.

McDonald MG, Harbaugh AW. 1988. A modular three-dimensional finite difference groundwater flow model. OR-83-875 U.S. Geological Survey, Reston, Virginia.

Moore RD, Sutherland P, Gomi T, Dhakal A. 2005. Thermal regime of a headwater stream within a clear-cut, coastal British Columbia, Canada. *Hydrological Processes* **19**: 2591–2608.

Packman AI, Salehin M. 2003. Relative roles of stream flow and sedimentary conditions in controlling hyporheic exchange. *Hydrobiologia* **494**: 291–297.

Peterson EW, Sickbert TB. 2006. Stream water bypass through a meander neck, laterally extending the hyporheic zone. *Hydrogeology Journal* **14**: 1443–1451, DOI: 10·1007/s10040-006-0050-3.

Portland General Electric (PGE). 2005. Application for Certification Pursuant to Section 401 of the Federal Clean Water Act. FERC No. 2195, Portland General Electric: Portland, Oregon, USA.

Polehn RA, Kinsel WC. 1997. Transient temperature solution for streamflow from a controlled temperature source. *Water Resources Research* **33**: 261–265.

Pollack DW. 1994. *User's Guide for MODFLOW/MODPATH-PLOT, version 3, A Particle Tracking Post-processing Package for MODFLOW, the U.S. Geological Survey Finite-difference Groundwater Flow Model*. U.S. Geological Survey: Reston, VA.

Poole GC, Berman CH. 2001. An ecological perspective on in-stream temperature: natural heat dynamics and mechanisms of human-caused thermal degradation. *Environmental Management* **27**: 787–802, DOI: 10·1007/s002670010188.

Poole GC, Stanford JA, Running SW, Frissell CA. 2006. Multiscale geomorphic drivers of groundwater flow paths: Subsurface hydrologic dynamics and hyporheic habitat diversity. *Journal of the North American Benthological Society* **25**: 288–303.

Silliman SE, Booth DF. 1993. Analysis of time-series measurements of sediment temperature for identification of gaining vs. losing portions of Juday Creek, Indiana. *Journal of Hydrology* **146**: 131–148.

Silliman SE, Ramirez J, McCabe RL. 1995. Quantifying downflow through creek sediments using temperature time series: one-dimensional solution incorporating measured surface temperature. *Journal of Hydrology* **167**: 99–119.

Sliva L, Williams DD. 2005. Exploration of riffle-scale interactions between abiotic variables and microbial assemblages in the hyporheic zone. *Canadian Journal of Fisheries and Aquatic Sciences* **62**: 276–290.

Stallman RW. 1965. Steady one-dimensional fluid flow in a semi-infinite porous medium with sinusoidal surface temperature. *Journal of Geophysical Research* **70**: 2821–2827.

Story A, Moore RD, Macdonald JS. 2003. Stream temperatures in two shaded reaches below cutblocks and logging roads: downstream cooling linked to subsurface hydrology. *Canadian Journal of Forest Research* **33**: 1383–1396, DOI: 10·1139/X03-087.

Sullivan K, Adams TN. 1991. The physics of stream heating: 2) An analysis of temperature patterns in stream environments based on physical principles and field data. Weyerhaeuser: Tacoma, Washington, USA. Technical Report 044-5002/89/2.

Torgersen CE, Price DM, Li HW, McIntosh BA. 1999. Multiscale thermal refugia and stream habitat associations of Chinook salmon in northeastern Oregon. *Ecological Applications* **9**: 301–319.

Wampler PJ. 2004. Contrasting geomorphic responses to climatic, anthropogenic, and fluvial change across modern to millennial time scales, Clackamas River. PhD Dissertation, Oregon State University, Oregon, 398.

Wondzell SM, Swanson FJ. 1999. Flood, channel change, and the hyporheic zone. *Water Resources Research* **35**: 555–567.